Measurements of Regional Ventilation Pulmonary Gas Volume: Theory and Error Analysis with Special Reference to Positron Emission Tomography

Sven O. Valind, Christopher G. Rhodes, Lars H. Brudin, and Terry Jones

MRC Cyclotron Unit and Department of Medicine, Royal Postgraduate Medical School, Hammersmith Hospital, London and Department of Clinical Physiology, University of Lund, Sweden

The adaptation to PET of the steady-state technique for the measurement of alveolar ventilation, based on the short-lived radionuclide ^{19}Ne ($T_{1/2}$ = 17.4 sec), allows the steady-state lung model to be analyzed in a quantitative way under well-defined geometrical conditions. The regional gas volume is essential to this analysis, and regional measurements of the pulmonary gas volume based on transmission tomography are presented and validated in this paper. The accuracy of the steady-state method rests largely with the validity of the lung model applied to describe the transport of tracer in the lung. This study considers tracer transport and mixing within individual lung regions. Blood flow and the alveolar-to-capillary exchange of gases do not significantly affect the values obtained, not even in regions with highly abnormal ventilation/perfusion ratios. A nonuniform intra-regional gas flow distribution results in an underestimation of the regional ventilation, determined by the dispersion of the ventilatory turnover rates of alveolar gas within the region. In the normal lung this underestimation is negligible. In disease, a mixing within the resolution volume of units that are almost non-ventilated and units that perform normally may result in an understimation of alveolar ventilation by up to 60%.

J Nucl Med 1991; 32:1937–1944

During the continuous inhalation of an inert-gas radionuclide, the alveolar concentration of isotope is determined by the turnover rate of alveolar gas and by radioactive decay. This concept was applied by Fazio and Jones for the steady-state imaging of regional ventilation using ^{81m}Kr and the gamma camera (*1*). In the present paper we describe the quantitative measurement of alveolar ventilation based on the adaption of the steady-state method to PET and the short-lived positron emitter ^{19}Ne ($T_{1/2}$ = 17.4 sec), earlier used in a qualitative manner by Crouzel et al. (*2*).

Received Feb. 29, 1991; revision accepted May 9, 1991.

For reprints contact: Sven O. Valind, Department of Clinical Physiology, University Hospital, S-221 85 LUND, Sweden.

With PET the regional concentration of isotope with respect to thoracic volume can be accurately measured in tomographic sections of the chest. Both the thoracic concentration of tracer (radioactivity per unit volume of thorax) and the pulmonary gas volume (ml of gas per unit volume of the thorax) may be obtained. The regional pulmonary gas volume represents a useful phsyiological parameter in its own right and it is also essential to the analysis of the steady-state lung model since it defines the distribution volume of insoluble gas tracers in the lung.

The purpose of this paper is to examine the accuracy afforded by the steady-state method for the measurement of the regional inspiratory minute ventilation of fresh gas. The accuracy is to some extent limited by the nature of the transport of diffusable tracers in the lung. The inter-regional distribution of tracer has been analyzed previously (*3*) where special considerations were given to the tidal breathing pattern and the reinspiration of mixed alveolar gas from the airways' dead space. This report addresses the intra-regional transfer of tracer, particularly the influence of intra-regional gas flow heterogeneities and the effects of gas transfer across the alveolar-capillary membrane. The statistical uncertainty of the measurements, due to the radioactive decay counting statistics, has been assessed together with the propagation of statistical noise, which arises when the measured parameters are converted into values of regional ventilation. Furthermore, values of the regional pulmonary gas volume, derived from transmission mode measurements of lung density, have been validated in vivo by emission tomography following the labeling of pulmonary gas with the long-lived positron emitter ^{13}N ($T_{1/2}$ = 10.0 min).

SUMMARY OF SYMBOLS

If not indicated otherwise, symbols relate to regional values of the parameters. For the time dependent parameters, the value at time t has been indicated by the inclusion of "(t)" after the symbol. The symbol without affix denotes the time-weighted average, which includes numerous

breathing cycles. Volumes of thoracic space are expressed in cm^3 while gas volumes are given in ml at BTPS (body temperature, ambient pressure, saturated with water vapor).

C_A = tracer concentration in alveolar gas ($MBq \cdot ml^{-1}$)
$\bar{C}_A$ = gas volume weighted mean of C_A for a given region of the thorax
C_{Th} = thoracic concentration of the tracer ($MBq \cdot cm^{-3}$)
C_I = concentration of tracer in inspired air ($MBq \cdot ml^{-1}$)
D_L = lung density expressed as tissue mass (including blood) per unit volume of thorax ($g \cdot cm^{-3}$)
λ_D = radioactive decay constant
λ_S = Ostwald solubility coefficient
$\dot{Q}$ = pulmonary blood flow per unit volume of thorax ($ml \cdot min^{-1} \cdot cm^{-3}$)
ρ_t = density of gas free lung tissue ($1.04\ g \cdot ch^{-3}$)
V_G = regional pulmonary gas volume expressed as gas volume per unit volume of thorax ($ml \cdot cm^{-3}$)
V_A = regional alveolar gas volume ($ml \cdot cm^{-3}$)
$\dot{V}_A$ = regional alveolar ventilation defined by the inspiratory minute ventilation of fresh gas per unit volume of thorax ($ml \cdot min^{-1} \cdot cm^{-3}$)
$\dot{V}_A/V_A$ = specific alveolar ventilation defined by the alveolar ventilation per unit volume of alveolar gas (min^{-1})

THEORY

The Steady-State Ventilation Model

The lung model used to analyze the steady-state alveolar concentration of the tracer (C_A) has been characterized by Amis and Jones in its application to ^{81m}kr (*4*). The model postulates that the net transport of tracer is determined by the alveolar ventilation ($\dot{V}_A$), which is expressed as a constant time independent gas flow to regions ventilated in parallel. Each region is assumed to be uniform with respect to tracer concentration, following complete mixing between inspired air and alveolar gas.

At equilibrium, the delivery of tracer by inspiration is balanced by the expiratory clearance and the radioactive decay, such that

$$C_A\dot{V}_A = C_A\dot{V}_A + \lambda_D C_A V_A \qquad \text{Eq. 1}$$

The isotope concentration in alveolar gas is obtained as the concentration per unit volume of thorax (C_{Th}) divided by the alveolar gas volume (V_A). Substituting for C_A, Equation 1 can be rearranged to give the operational equation of the model:

$$\dot{V}_A = \frac{\lambda_D V_A}{\frac{C_I V_A}{C_{Th}} - 1} \qquad \text{Eq. 2}$$

Intra-Regional Tracer Transport and Gas Mixing

The steady-state lung model relies on a close correlation between tracer transport and the convective flow of fresh gas. Mechanisms underlying the transfer of gas during inspiration, however, change along the bronchial tree. The interaction between convective flow and diffusion results in an axial concentration front between inspired air and alveolar gas—the stationary alveolar interface. With the inspiratory flow rates encountered in normal lung during quiet breathing, this interface extends from the 15th airway generation in the distal direction (*5,6*). In airways proximal to the concentration front, convective transport dominates while gas transport is largely diffusion-dependent distal to the 15th airway generation, i.e., in regions subtended by terminal bronchioles (acinar units). Similar conditions should also hold for ^{19}Ne with diffusive properties in the gas phase close to those of nitrogen and oxygen. The delivery of tracer to the lung regions considered, i.e., to regions subtended by the 7–8th airway generations (see METHODS), thus follows the convective inspiratory gas flow. Similarly, the amount of ^{19}Ne expelled from such a region is determined by the convective expiratory flow, but only if the intra-regional mixing between inspired air and alveolar gas is complete.

Diffusion provides an efficient gas mixing within acini in the normal lung (*7*), but the intra-regional tracer concentration may vary due to differences in gas flow between acini. In diseases, significant tracer concentration gradients may develop, even at the intra-acinar level. An uneven intra-regional gas flow distribution serves to increase the amount of tracer expelled since the expiratory clearance would be biased towards the better ventilated parts, which hold the higher levels of tracer concentration. The regional content of ^{19}Ne will be reduced and the average alveolar concentration of ^{19}Ne in the region ($\bar{C}_A$) is determined by the coefficient of variation (COV_s) of the intra-regional dispersion of the ventilatory turnover rates of alveolar gas (ventilation per unit alveolar gas volume) such that:

$$\frac{\bar{C}_A}{C_A} = 1 - (COV_s)^2 \cdot \frac{\lambda_D \dot{V}_A/V_A}{(\lambda_D + \dot{V}_A/V_A)^2} \qquad \text{Eq. 3}$$

where C_A is the concentration that would be encountered if the gas flow distribution was uniform. $\dot{V}_A$ is the total ventilation of the region and V_A denotes its gas volume. Values of regional ventilation obtained are based on measurements of $\bar{C}_A$. Therefore, an uneven intra-regional gas flow distribution results in an underestimation of $\dot{V}_A$.

Alveolar-Capillary Gas Exchange

Although the solubility of neon is low ($\lambda_{S(Ne)} = 0.0097$, (*8*)), small amounts of ^{19}Ne will be cleared by blood flow ($\dot{Q}$). Furthermore, the alveolar exchange of oxygen and carbon dioxide is blood flow dependent and results in a net transfer of gas so that the expired minute ventilation ($\dot{V}_{AE}$) generally differs from the inspired minute ventilation ($\dot{A}_{AI}$), as indicated by the respiratory exchange ratio (RQ). The resulting mass balance equation with respect to ^{19}Ne may be written such:

$$C_I\dot{V}_{AI} = C_A\dot{V}_{AE} + \lambda_{S(Ne)} C_A\dot{Q} + \lambda_D C_A V_A \qquad \text{Eq. 4}$$

The net transfer of tracer due to dead space ventilation plays little role in this analysis and has been omitted. The concentration of tracer in mixed venous blood is considered to be negligible due to the short half-life of ^{19}Ne. Equation 4 can be rearranged to give

$$\dot{V}_{AI} = \frac{\lambda_D V_A}{\frac{C_I}{C_A}} - K_{Ne} \qquad \text{Eq. 5}$$

This may differ from the operational equation of the steady-state method (Eq. 2) subject to the value of K_{Ne}, which is given by

$$K_{Ne} = \frac{\dot{V}_{AE}}{V_{AI}} + \frac{\lambda_{S(Ne)}}{V_{AI}/Q} \qquad \text{Eq. 6}$$

K_{Ne} may be rewritten to $(\dot{V}_{AE} + \lambda_{S(Ne)}\dot{Q})/\dot{V}_{AI}$, which is the ratio of the clearance of tracer by way of transport (expiratory gas flow and blood flow) to the clearance that would be encountered if there was no gas transfer across the alveolar-capillary membrane or, equivalently, if the region considered was non-perfused.

Delivery of Tracer

The steady-state method relies on the continuous supply of tracer at constant concentration in inspired air and the inspired ^{19}Ne concentration $C_I(t)$ was monitored continuously during the recordings of tomograms. A breath to breath variation in $C_I(t)$ invalidates the assumption of steady-state conditions and errors arise when Equation 2 is used to calculate alveolar ventilation. The rate of change of the regional ^{19}Ne content is determined by the difference between delivery and clearance of tracer and the tracer concentration in alveolar gas at a given time $C_A(t)$ may be derived from the mass balance equation

$$\left(\frac{d}{dt} C_A(t)\right)V_A = C_I(t)\dot{V}_A - C_A(t)\dot{V}_A - \lambda_D C_A(t)V_A \qquad \text{Eq. 7}$$

when $C_I(t)$ and $\dot{V}_A/V_A$ are known. $C_A(t)$ will approach the actual steady-state level with a time constant equal to $\lambda_D + \dot{V}_A/V_A$ as $C_I(t)$ varies.

The measured values of tracer concentration in inspired air and in alveolar gas relate to the time weighted average of the parameters, which were calculated for the seven min scanning period. The resulting values of alveolar ventilations obtained by the use of Equation 2 were then compared with the predefined values.

Measurements of the Regional Pulmonary Gas Volume

The regional lung tissue density (D_L) is determined by the relative amounts of gas and tissue per unit volume of the thorax. The regional volume of lung tissue (including blood, interstitial and alveolar structures and fluid) equals D_L/ρ_t, where ρ_t denotes the density of gas free lung tissue (1.04 $g \cdot cm^{-3}$). The regional gas volume ($V_{G(D)}$) may thus be calculated such

$$V_{G(D)} = 1 - \frac{D_L}{\rho_t} \qquad \text{Eq. 8}$$

expressed in ml gas (BTPS) per cm^3 of thorax.

The regional lung density is obtained from the transmission mode measurement. Rhodes et al. (*9*) demonstrated a slight overestimation of density in low density objects, when surrounded by a high-density photon scattering medium (e.g., water). In the thorax, the influence of the chestwall and mediastinal structures thus are expected to result in a small overestimation of D_L. Measured in a chest phantom, the density of "lung" regions containing air alone was found to be overestimated by 0.026 $g \cdot cm^{-3}$ on average (range 0.017 to 0.035 $g \cdot cm^{-3}$). To compensate for this small systematic error, a value of 0.026 $g \cdot cm^{-3}$ has been subtracted from the transmission tomogram.

An alternative method to measure the regional pulmonary gas volume is based on the labeling of pulmonary gas with the long lived isotope nitrogen-13 ($T_{1/2}$ = 10.0 min). Owing to the low solubility of nitrogen [the blood/gas partition coefficient equals 0.015 at body temperature (*10*)], the distribution volume of inhaled ^{13}N (denoted by $V_{G(13N)}$) is close to the pulmonary gas volume. At equilibrium, the concentration of ^{13}N in the pulmonary gas phase ($C_{Th}/V_{G(13N)}$) equals the concentration in inspired air (C_I). Hence,

$$V_{G(13N)} = \frac{C_{Th}}{C_I} \qquad \text{Eq. 9}$$

which allows the regional pulmonary gas volume to be calculated as the thoracic to input ^{13}N concentration ratio.

Statistical Errors

The random errors of the measured values of ^{19}Ne input concentration typically amount to some 0.2% for a total number of 0.2–0.3 × 10^6 counts recorded. For the tomographic measurements, the relationship between the number of counts and the statistical uncertainty is complex. The primary observations (i.e., the number of coincidence events for the detector pairs) are Poisson distributed, but the statistical errors of individual regions in the tomogram are influenced by the image reconstruction process. For emission tomograms the COV of the measured values of isotope concentration in a resolution element may be estimated from the total number of counts recorded, revised for the enhancement of statistical noise associated with the correlation of photon attenuation using transmission mode data (*11,12*).

When calculating values of alveolar ventilation, the relationship between alveolar ventilation and the measured parameters results in an amplification of the statistical

noise, expressed by

$$COV_{\dot{V}_A} = \left[\left(\frac{\dot{V}_A/V_A}{\lambda_D}\right)^2 \cdot (COV_{V_{G(D)}})^2 + \left(1 + \frac{\dot{V}_A/V_A}{\lambda_D}\right)^2 \cdot (COV_{Ne})^2\right]^{1/2} \quad \text{Eq. 10}$$

in the conventional first order approximation (*13*). When presented as specific alveolar ventilation ($\dot{V}_A/V_A$), the results are slightly more sensitive to noise in the measurement of alveolar volume and

$$COV_{\dot{V}_A/V_A} = \left(1 + \frac{\dot{V}_A/V_A}{\lambda_D}\right)[(COV_{V_{G(D)}})^2 + (COV_{Ne})^2]^{1/2} \quad \text{Eq. 11}$$

METHODS

Instrumentation

Measurements were made using an ECAT II instrument (CTI, Knoxville) in the emission and transmission modes (*14*). The spatial resolution of the instrument, measured as the full width at half maximum response to a line source of radioactivity surrounded by water (FWHM) is 1.7 cm in all directions. In the axial direction, this defines the thickness of the tomographic section.

In the lung, the effective FWHM tends to increase due to the penetration of positrons through gas-filled alveoli prior to annihilation. The penetration distance, which is determined by the positron energy and the density of the absorbing medium (*15*), is negligible in solid tissue (*16*). In regions with a lung density of 0.40 $g \cdot cm^{-3}$, however, only 50% of positrons emitted from ^{19}Ne are annihilated within a distance of 0.35 cm from the isotope and this distance is increased to 0.70 cm in regions with a density of 0.20 $g \cdot cm^{-3}$. The resulting effective spatial resolution is 1.9 and 2.3 cm FWHM respectively. These values are representative of the normal lung. In emphysematous lung spatial resolution may deteriorate with a calculated FWHM of 4.8 cm in regions with a lung density of 0.05 $g \cdot cm^{-3}$.

In normal lung, the resolution element of the tomogram [defined by a square with the side equal to the FWHM (*11*)] covers an area of approximately 2 × 2 cm^2 in the tomographic plane. The values of isotope concentration obtained for this region are influenced by isotope in surrounding lung as a result of the limited spatial resolution. At a distance of ½ FWHM from a point source of radioactivity, the weighting factor has decreased to half and amounts to a few percent only at a distance equal to the FWHM. For a resolution of 2.0 cm in all directions, a lung region reaching 1/2 FWHM outside the resolution element covers some 4 × 4 cm^2 in the tomographic plane and an axial distance of 2 cm. Such a region corresponds to the volume of some 100–200 acinar units (0.5%–1.0% of the entire lung) i.e., to a lung region subtended by airways of the 7–8th airway generation.

Gas Volume Measurements

Seven normal healthy subjects were studied in the supine position. The level of the single transverse tomographic plane was chosen from the caudal part of the lung, well clear of the diaphragm. A 10–15-min transmission scan including some ten million coincidence events was recorded, using an external radiation source encircling the subject. Following this, the pulmonary gas phase was labeled with ^{13}N, produced in a cyclotron by the $^{12}C(d,n)^{13}N$ reaction (*17*). Nitrogen-13 was continuously supplied from a 50-ml batch using a Harvard constant infusion pump, mixed with a constant air flow and fed to an anaesthetic balloon from which the subject inhaled via a mouthpiece and a one-way valve. Gas was continuously sampled from the outlet of the balloon and the sec to sec variation in ^{13}N input concentration monitored using a NaI-detector, cross calibrated with the tomograph. The input concentrations was adjusted to BTPS conditions to be compatible with the measured isotope concentration in the lung. Of the 13-min tracer administration time, the first 5 min were allowed for equilibration. The time was chosen for the tracer to equilibrate also in low ventilation regions, which, in the normal lung, have a gas turnover rate of some 1.0 min^{-1} during quiet breathing.

The amount of ^{13}N delivered was some 3 GBq (80 mCi), which resulted in the accumulation of 0.8–1.2 × 10^6 coincidence events and an absorbed dose of 0.8 mGy in the lung. During the transmission scan, the radiation exposure of 0.2 mGy is confined to the lung section being scanned.

The lung density tomogram is also used to delineate the lung. Due to the finite spatial resolution of the detector system, the lung-to-chestwall interface will be represented by a gradual change in density (Fig. 1). The lower end of this gradient was used to outline the lung. In this way some 2 cm of peripheral lung will be excluded from the analysis in order to avoid influence from the chestwall. The analysis was made in regions of 2 × 2 cm^2 covering the delineated lung fields. In most subjects the area of the left lung field in the tomogram was less than half the area of the right lung. This leaves a considerably smaller spatial range for systematic topographical differences to be observed in the left lung and the topographical analysis was therefore confined to the right lung.

Neon-19 Tomograms

Measurements of ventilation referred to in this paper represent clinical studies of normal subjects and patients with lung disease. The full details of these studies will be presented elsewhere.

Subjects were studied in supine position. During the inhalation of ^{19}Ne a period of 2–3 min was allowed for equilibration before recording of the 400 sec emission scan, resulting in the accumulation of 0.4 to 0.8 × 10^6 coincidence events.

Neon-19 was produced on line by the $^{16}O(\alpha,n)^{19}Ne$ reaction (*2*) diluted with air to provide a gas flow of 10–12 liters per min and delivered to the patient by the same dispensing system that was used for ^{13}N.

RESULTS

Gas Volume Measurements

The density image (Fig. 1) demonstrates the anatomical structure of the thoracic section, where the mediastinum, spine and chestwall form the high density (1.0–1.2 $g \cdot cm^{-3}$) regions. Tomograms of the pulmonary gas volume derived from lung density ($V_{G(D)}$) and nitrogen-13 ($V_{G(13N)}$) are presented in Figure 2. The analyzed area of the right lung field, ranged from 56–88 cm^2 in the 7 subjects.

To study any overall differences between the two methods, the mean gas volume was calculated for the right and left lung fields for each subject (Fig. 3). In the right lung

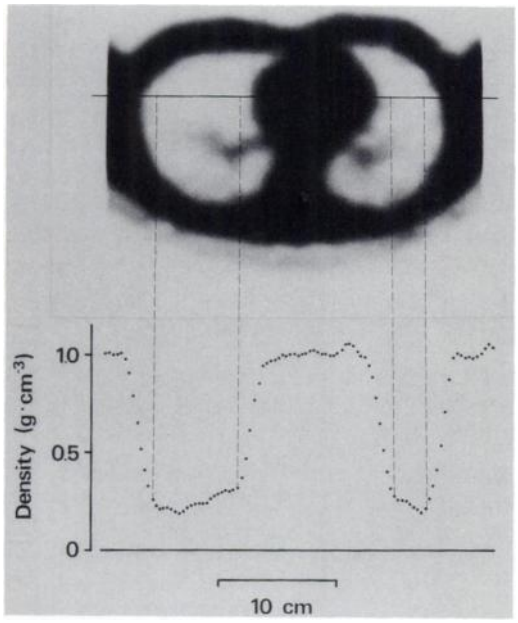

FIGURE 1. Density profile through the chest at the horizontal level indicated in the density tomogram. There is a gradual change in density from 0.2–0.4 g·cm^{-3} in the lung to 1.1–1.2 g·cm^{-3} in the chestwall, covering a distance of approximately twice the FWHM.

the mean $V_{G(13N)}$ in the seven subjects was on average 0.715 ml gas per cm^3 of thorax. $V_{G(D)}$ was slightly lower (0.703 ml·cm^3) but the difference was not statistically significant ($p > 0.3$ paired T-test). In the left lung, however, $V_{G(13N)}$ (0.678 ml·cm^{-3}) was 7.5% higher than $V_{G(D)}$ (0.631 ml·cm^{-3}) ($p < 0.02$).

There is a topographical variation in the pulmonary gas volume and $V_{G(13N)}$ varied from 0.708–0.832 ml·cm^{-3} in ventral parts of the right lung in the seven subjects to 0.563–0.715 ml·cm^{-3} in dorsal parts. Possible topographical differences between $V_{G(D)}$ and $V_{G(13N)}$ were studied in a ventro-dorsal strip of the right lung (Fig. 3), but no systematic differences between $V_{G(13N)}$ and $V_{G(D)}$ were to be found at any gravitational level ($p > 0.1$ analysis of variance).

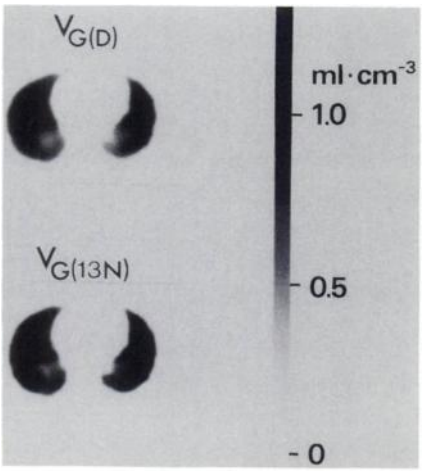

FIGURE 2. Tomograms of the pulmonary gas volume in a section some 5–7 cm cranial to the diaphragm. The subject is in the supine posture and viewed in the foot-to-head direction. The images illustrate the pulmonary gas volume as calculated from lung density (upper panel) and nitrogen-13 (lower panel).

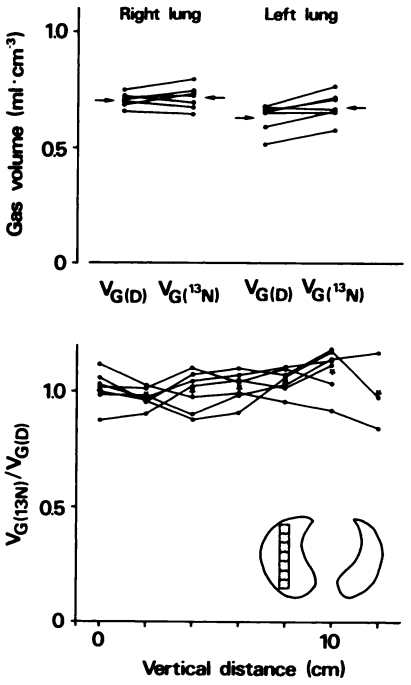

FIGURE 3. The average fractional gas volume in the right and left lung fields of the seven subjects, as calculated from lung density ($V_{G(D)}$) and nitrogen-13 ($V_{G(13N)}$)—upper panel. The mean values are indicated by arrows. Individual vertical profiles of $V_{G(13N)}/V_{G(D)}$ in regions 2 × 2 cm^2 (see insert)—lower panel. The mean value at each level has been indicated (*).

Neon-19 Transport

Delivery. Equation 7 was solved for different temporal patterns in the changes of $C_I(t)$ (step function, linear slope and sinusoidal with a period in the range 1–14 min). $\dot{V}_A/V_A$ was assigned values in the range 0.1–4.0 min^{-1}. Even if the peak-to-peak variations in $C_I(t)$ during the acquisition of tomograms amount to some 30% of the mean level, errors do not exceed 2.5%. In practice, $C_I(t)$ was stable within ± 10% during the scanning procedure in most cases, but a peak-to-peak variation of the order of 25% of the mean level was observed in a few subjects. The variability of C_I was mainly the result of fluctuations in the cyclotron α-particle beam current, with a time course extending over several breaths. Systematic variations in C_I within the respiratory cycle could affect the regional distribution of tracer, but only to the extent different regions are inflated in sequence. However, no such variations were observed within the limits of the C_I sampling time resolution (1.0 sec).

Intra-Regional Heterogeneity. The flow distribution in disease may be highly irregular and the largest errors will arise in regions with a bimodal distribution, comprising two populations of alveoli only. At the extreme, this could theoretically result in an underestimation of $\dot{V}_A$ by some 60% (Fig. 4) when some units are virtually non-ventilated while gas flow in remaining parts of the region is normal or increased. Such a functional separation of units within the resolution element of the tomogram, would imply that this small volume (comprising some 0.5%–1.0% of the total lung) consists solely of units which are either severely affected by disease and almost non-ventilated or virtually unaffected and perform normally.

For a unimodal gas flow distribution, in contrast, the

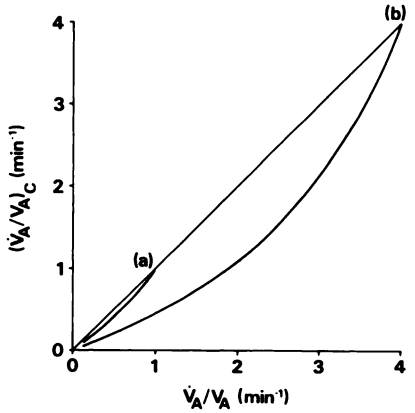

FIGURE 4. Cal-culated values of regional ventilation $(\dot{V}_A/V_A)_C$ based on the volume weighted average ^{19}Ne concentration in a region with heterogeneous gas flow distribution. V_A denotes the regional gas volume and $\dot{V}_A$ the actual ventilation of the region. For any given value of $\dot{V}_A/V_A$ the graphs represent the worst possible case, i.e., a bimodal flow distribution where the modes represent the extremes of a given range of specific alveolar ventilation within the region: 0–1.0 min^{-1} (a) and 0–4.0 min^{-1} (b). The relative volume of ventilated to unventilated units is determined by $\dot{V}_A/V_A$ in each case. The thin line indicates the line of identity.

errors are considerably smaller even when there is a large range in ventilatory turnover rate between better ventilated units and the low ventilation units within the region considered (Fig. 5). The underestimation of $\dot{V}_A$ caused by an uneven intra-regional gas flow distribution with a COV_s of 0.33, does not exceed 6.5% when $\dot{V}_A/V_A$ is in the range 0.1–4.0 min^{-1}.

Alveolar-Capillary Gas Exchange. The ratio of expired to inspired minute ventilation $\dot{V}_{AE}/\dot{V}_{AI}$ and, thus, the value of K_{Ne}, may be calculated from the composition of alveolar gas, which is determined by the regional ventilation/perfusion ratio (*18*). Regions with a normal $\dot{V}_{AI}//\dot{Q}$ (around 0.7) K_{Ne} are close to unity. The gas volume expired is indeed some 1.5% lower than the volume inspired, but this small reduction in the amount of tracer expelled is balanced for by the removal of ^{19}Ne dissolved in blood, leaving the net transport of ^{19}Ne virtually unaffected.

If ventilation deteriorates, regions with abnormally low ventilation/perfusion ratios may appear. For a regional $\dot{V}_{AI}/\dot{Q}$ equal to 0.05, $\dot{V}_{AE}$ is some 10% lower than $\dot{V}_{AI}$ and the ventilatory clearance of tracer is reduced accordingly. Even so, the amount of ^{19}Ne removed is *enhanced* by some 9% (K_{NE} = 1.09) due to ^{19}Ne cleared by blood flow. This increase, however, is of minor significance, since the overall clearance of ^{19}Ne becomes progressively dependent on radioactive decay as ventilation goes down ($K_{Ne} \ll CI/CA$) and the values of regional ventilation obtained using Equation 2, do not deviate from $\dot{V}_{AI}$ by more than 1%.

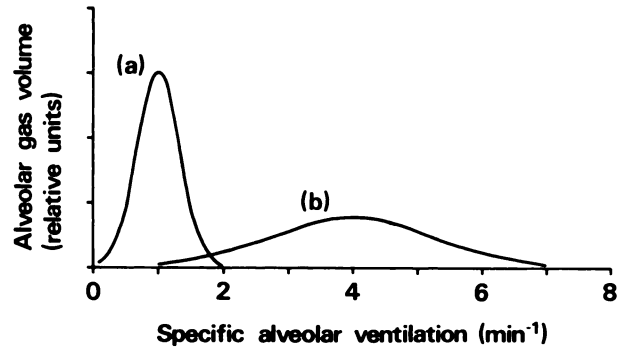

FIGURE 5. Illustrations of the volume distribution of the specific alveolar ventilation in regions where the gas flow distribution follows a gaussian frequency function with a coefficient of variation equal to 0.33. This heterogeneity results in an underestimation of the actual regional ventilation ($\dot{V}_A$) by 3.2% in a region with $\dot{V}_A/V_A$ equal to 1.0 min^{-1} (a) and by 6.5% in a region with $\dot{V}_A/V_A$ equal to 4.0 min^{-1} (b).

Statistical Errors

In the normal lung, the calculated COV_{Ne} amounts to some 2–3% for the 0.4 to 0.8 × 10^6 counts acquired in the ^{19}Ne tomogram.

The statistical errors increase in regions of low ventilation due to the low concentration of ^{19}Ne in such regions. For a ventilation of 0.2 min^{-1}, commonly found in patients with severe obstructive lung disease, COV_{Ne} equals 10–12%.

The statistical uncertainty of $V_{G(D)}$ was obtained from phantom studies using a chest phantom with a "lung" density of 0.25 ml·cm^{-3} in repeated transmission mode measurements. Each tomogram contained ten million counts, conditions which are representative of the human studies, resulting in a $COV_{V_{G(D)}}$ of 3.5%.

The statistical precision of the values and $\dot{V}_A$ and $\dot{V}_A/V_A$ obtained deteriorates in regions of very high ventilation due to the enhancement of noise, and in regions of very low ventilation due to the relatively high statistical uncertainty associated with the measurement of low ^{19}Ne concentration (Fig. 6).

DISCUSSION

Pulmonary Gas Volume

The methods used to measure the regional pulmonary gas volume refer to the two complementary compartments in the lung, tissue, and gas. The measurements in that transmission mode data are both used to calculate $V_{G(D)}$ and to correct the ^{13}N emission tomogram for the absorption of photons in the chest. Errors in the transmission mode measurement are therefore propagated into the attenuation correction of the ^{13}N tomogram. However, an overestimation of photon attenuation and, consequently of D_L, serves to underestimate $V_{G(D)}$ while the ^{13}N thoracic concentration and $V_{G(13N)}$ is overestimated. Thus, the coupling of the measurements tends to amplify possible differences between $V_{G(D)}$ and $V_{G(13N)}$, rather than to cause false-positive correlations.

The transmission measurement is routinely made for the attenuation correction of emission tomograms and forms a prerequisite for all PET studies of the chest. The

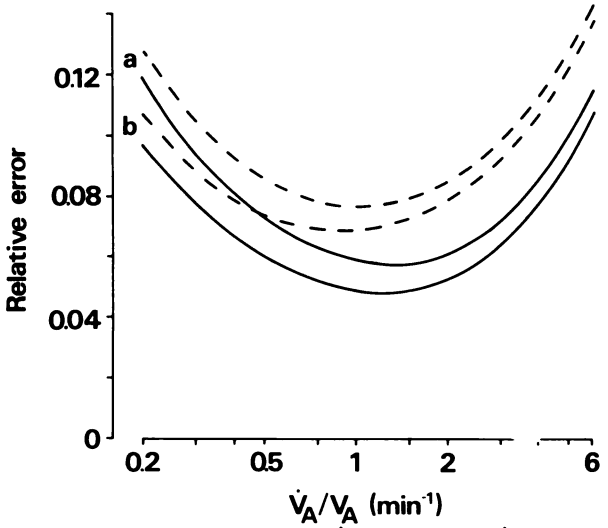

FIGURE 6. Relative errors in $\dot{V}_A$ (——) and $\dot{V}_A/V_A$ (- - -) caused by statistical noise in the measured parameters, for different values of $\dot{V}_A/V_A$. The total number of counts assigned to the ^{19}Ne and the transmission tomograms were 0.5×10^6 and 10×10^6 respectively. Two different values of V_A were considered, 0.60 ml·cm^{-3} (a) and 0.80 ml·cm^{-3} (b).

calculation of $V_{G(D)}$ relies on the proportionality between the transmission object/blank tomogram and object density, valid for homogenous objects. In the lung, the influence from surrounding structures serves for density to be slightly overestimated, but with the small correction applied (0.026 ml·cm^{-3}) no significant differences were found between $V_{G(D)}$ and $V_{G(13N)}$ in the right lung field of the section through the caudal third of the lung. At this level of the thorax, $V_{G(D)}$ slightly underestimates the pulmonary gas volume in the left lung field, possibly subject to differences in detection geometry between the left and right lung fields.

The measurement of $V_{G(13N)}$ relies on the equilibration of tracer between alveolar gas and inspired air. The alveolar concentration of ^{13}N, however, generally differs from the inspired concentration subject to the influence of blood flow on tracer transport, as earlier discussed for ^{19}Ne.

In the normal lung ($\dot{V}_{AI}/\dot{Q}$ around 0.7) the difference between alveolar (C_A) and input concentration (C_I) is negligible. For a $\dot{V}_{AI}/\dot{Q}$ equal to 0.05, C_A is some 17% lower than C_I and $V_{G(13N)}$, as calculated from Equation 4, underestimates the actual pulmonary gas volume by a similar number. Furthermore, in patients with obstructive lung disease, regions with very low ventilation are likely to exist and steady-state conditions may be impossible to achieve due to the extended equilibration time needed. Thus, the small gain in accuracy expected by a separate labeling of pulmonary gas using ^{13}N is questionable, except in normal lung.

Regional Ventilation

The aveolar concentration of ^{19}Ne is a slightly ambiguous indicator of ventilation in the sense that ventilation refers to the mechanical aspects of gas flow rather than to the transport of a specific gas. The tidal nature of gas transport may cause substantial variations in the alveolar ^{19}Ne concentration in the course of a single breath, but the measured average level of ^{19}Ne during numerous breathing cycles is determined by the net transfer of a tracer and is virtually unaffected by the breathing pattern per se (*3*). In a perfectly uniform lung only the fresh gas inspired ($\dot{V}_A$) contributes to the supply of tracer, but with the existence of regional differences in ventilation the reinspiration of mixed alveolar gas held by the airways' dead space at end-expiration results in a net transfer of tracer between regions. The airways dead space will also influence the measured values of ^{19}Ne concentration by way of tracer decay during transit through the bronchial tree, and the contribution by isotope in nonexchanging fresh gas held by the distal airways during inspiration.

In the normal lung, the errors $\dot{V}_A$ attributed to ventilation of the airways dead space range from an overestimation by some 3% in low ventilation regions ($\dot{V}_A/V_A$ = 1.0 min^{-1}) to an underestimation by some 8% in the better ventilated parts ($\dot{V}_A/V_A$ = 3.5 min^{-1}), as previously reported (*3*). In this context the errors caused by gas transfer across the alveolar-capillary membrane and by intra-regional gas flow heterogeneities, are negligible.

In disease, the intra-regional gas flow distribution is essentially unknown. Affected regions may suffer from a considerable degree of heterogeneity and $\dot{V}_A$ will be underestimated accordingly. In addition, errors associated with ventilation of the airways' dead space tend to increase as the regional ventilation falls, mainly as a result of tracer held by the distal airways, the influence of which is augmented because of the low alveolar concentration of ^{19}Ne in low ventilation regions. Thus, if $\dot{V}_A/V_A$ equals 0.1 min^{-1}, non-exchanging gas in airway generations 9–17 would impose an overestimation of $\dot{V}_A$, by almost a factor of 2 (*3*). However, the importance of these sources of errors is to some extent suppressed since tracer transport in distal airways becomes progressively diffusion dependent as the regional ventilation falls. The concentration interface is therefore shifted in the proximal direction and the volume of non-exchanging gas in affected regions tends to decrease. Furthermore, both diffusive and convective transport of tracer between units within the region considered, via the distal airways, serve to reduce any intra-regional tracer concentration gradients and, thus, to reduce the effects of intra-regional flow heterogeneities.

In conclusion, the ability to quantitate regional ventilation using the steady-state method is to some extent limited by the nature of gas transport in the human lung. This applies, however, to all methods based on diffusable tracers. The limitations attributable to the simplifications implied by the steady-state lung model do not severely affect the accuracy in normal lung during quiet breathing. Although the biological input to these sources of error is largely unknown in disease, it is evident that accuracy may

deteriorate in those instances where the regional ventilation is very low or the intra-regional gas flow distribution is markedly nonuniform.

ACKNOWLEDGMENTS

This study was supported jointly by the Swedish National Association against Chest and Heart Diseases, the Swedish Medical Research Council (grant number 02872) and the Medical Research Council of the United Kingdom. We wish to thank Mr. D.D. Vonberg and the staff of the MRC Cyclotron Unit for invaluable support and technical help, and all the volunteers for making this study possible.

REFERENCES

1. Fazio F, Jones T. Assessment of regional ventilation by continuous inhalation of radioactive kyrpton-81m. *Br Med J* 1975;3:673–675.
2. Crouzel C, Guenard H, Comar D, et al: A new radioisotope for lung ventilation studies: Neon-19. *Eur J Nucl Med* 1980;5:431–434.
3. Valind SO, Rhodes CG, Jonson B. Quantification of regional ventilation in man by means of a short-lived radiotracer—theoretical evaluation of the steady-state model. *J Nucl Med* 1987;28:1144–1154.
4. Amis TC, Jones T. Krypton-81m as a flow tracer in the lung: theory and quantitation. *Bull Eur Physiopath Resp* 1980;15:245–259.
5. Paiva M. Gas transport in the human lung. *J Appl Physiol* 1973;34:401–410.
6. Paiva M, Engel LA. Pulmonary interdependence of gas transport. *J Appl Physiol* 1979;47:296–305.
7. Paiva M, Engel LA. Model analysis of gas distribution within human lung acinus. *J Appl Physiol* 1984;56:418–425.
8. Seeman P. Membrane actions of anesthetics and tranquilizers. *Pharmacol Rev* 1972;24:583–655.
9. Rhodes CG, Wollmer P, Fazio F, et al. Quantitative measurement of regional extravascular lung density using positron emission and transmission tomography. 1981;5:783–791.
10. Van Slyke DD, Dillon RT, Margaria R. Studies of gas and electrolyte equilibria in blood: XXIII. Solubility and physical state of atmospheric nitrogen in blood cells and plasma. *J Biol Chem* 1934;105:571–596.
11. Budinger TF, Derenzo SE, Greenberg WL, et al. Quantitative potentials of dynamic emission computed tomography. *J Nucl Med* 1978;19:309–315.
12. Huang SC, Hoffman EJ, Phelps ME, et al. Quantitation in positron emission computed tomography. 2. Effects of inaccurate attenuation correction. *J Comput Assist Tomogr* 1979;3:804–814.
13. Armitage P. *Statistical methods in medical research.* Oxford: Blackwell Scientific Publications; 1983:96–98.
14. Phelps ME, Hoffman EJ, Huang SC, et al: ECAT: a new computerized tomographic imaging system for positron-emitting radiopharmaceuticals. *J Nucl Med* 1978;19:635–647.
15. Evans RD. *The atomic nucleus.* New York: McGraw-Hill; 1955:621–628.
16. Phelps M, Hoffman E, Huang H, et al. Effect of positron range on spatial resolution. *J Nucl Med* 1975;16:649–652.
17. Clark JC, Buckingham PD. *Short-lived radioactive gases for clinical use.* London: Butterworth & Co (Publishers) Ltd; 1975:171–214.
18. West JB, Wagner PD. Pulmonary gas exchange. In: *Bioengineering aspects of the lung.* New York-Basel; Marcel Dekker Inc; 1977:361–457.